NANO LETTERS

pubs.acs.org/NanoLett Letter

Flexible, Mechanically Robust, Solid-State Electrolyte Membrane with Conducting Oxide-Enhanced 3D Nanofiber Networks for Lithium Batteries

Mengmeng Zhang, Peng Pan, Zhongling Cheng, Jieting Mao, Liyuan Jiang, Changke Ni, Soyeon Park, Kaiyue Deng, Yi Hu,* and Kun Kelvin Fu*

Cite This: https://doi.org/10.1021/acs.nanolett.1c01704 Read Online

ACCESS | Metrics & More | Article Recommendations | Supporting Information

ABSTRACT: Using a three-dimensional (3D) Li-ion conducting ceramic network, such as $Li_7La_3Zr_2O_{12}$ (LLZO) garnet-type oxide conductor, has proved to be a promising strategy to form continuous Li ion transfer paths in a polymer-based composite. However, the 3D network produced by brittle ceramic conductor nanofibers fails to provide sufficient mechanical adaptability. In this manuscript, we reported a new 3D ion-conducting network, which is synthesized from highly loaded LLZO nanoparticles reinforced conducting polymer nanofibers, by creating a lightweight continuous and interconnected LLZO-enhanced 3D network to outperform conducting heavy and brittle ceramic nanofibers to offer a new design principle of composite electrolyte membrane featuring all-round properties in mechanical robustness, structural flexibility, high ionic conductivity, lightweight, and high surface area. This composite-nanofiber design overcomes the issues of using ceramic-only nanoparticles, nanowires, or nanofibers in polymer composite electrolyte, and our work can be considered as a new generation of composite electrolyte membrane in composite electrolyte development.

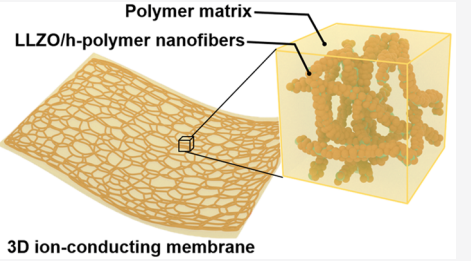

KEYWORDS: *Solid-state electrolyte, mechanical robustness, 3D conducting nanofibers, flexible membrane, polymer composite*

INTRODUCTION

Driven for high-energy density, research on lithium metal batteries has attracted widespread attention because of the highest specific capacity (3860 mA h g^{-1}) and the lowest electrochemical potential (−3.040 V vs the standard hydrogen electrode) of the lithium metal anode, which can maximize the capacity density and voltage window for increased battery energy density.[1−4] However, lithium metal batteries with liquid electrolytes exhibit serious dendrite growth problems.[5−8] The continuous growth of dendrites will consume the electrolyte and even pierce the separator, causing the battery to short-circuit, heat, and cause a risk of fire and explosion.[9−11] Although a lot of research has been done on these issues, dendrite growth and unstable SEI are inevitable due to the thermodynamic behavior of small molecules in organic solvents.[12−14] Replacing liquid organic electrolyte with solid electrolytes can eliminate side reactions between organic solvents and the Li-metal anode, and solid electrolytes have a higher mechanical modulus, which can inhibit dendrite growth and prevent puncture.[15−17] The use of lithium metal anodes in conjunction with lithium metal anodes can significantly improve battery safety.

Solid electrolytes mainly include organic polymers, inorganic materials, and organic−inorganic composite electrolytes. Composite electrolytes generally exhibit flexibility, high ionic conductivity, and good contact with the electrode. Previous studies showed that dispersing inorganic fillers (such as SiO_2,[18] ZrO_2,[19] TiO_2,[20] and other non-Li^+-conductive nanoparticles or $Li_7La_3Zr_2O_{12}$,[21] $Li_{0.33}La_{0.557}TiO_3$,[22] and other Li^+-conductive nanoparticles) in a polymer matrix can reinforce mechanical properties compared to pristine polymer electrolytes.[23−26] Moreover, the particles are incorporated into the polymer matrix to affect the recrystallization kinetics of the polymer chain, thereby promoting the local amorphous region and improving the ionic conductivity of the lithium salt polymer system.[27,28] Because of the increased area of the amorphous region and the improvement of the interface between filler and polymer, the development of nanostructured fillers has been proven as an effective ongoing strategy to improve ion conductivity of polymer composite electrolytes.[29−31] A representative work by Cui and co-workers[22] has demonstrated a one-dimensional nanowire fillers using $Li_{0.33}La_{0.557}TiO_3$, which is perovskite-type conductive lithium ion conductor, to enhance the bulk ionic conductivity of its polymer composite electrolyte. Such an improvement is contributed by the

Received: April 30, 2021
Revised: June 3, 2021

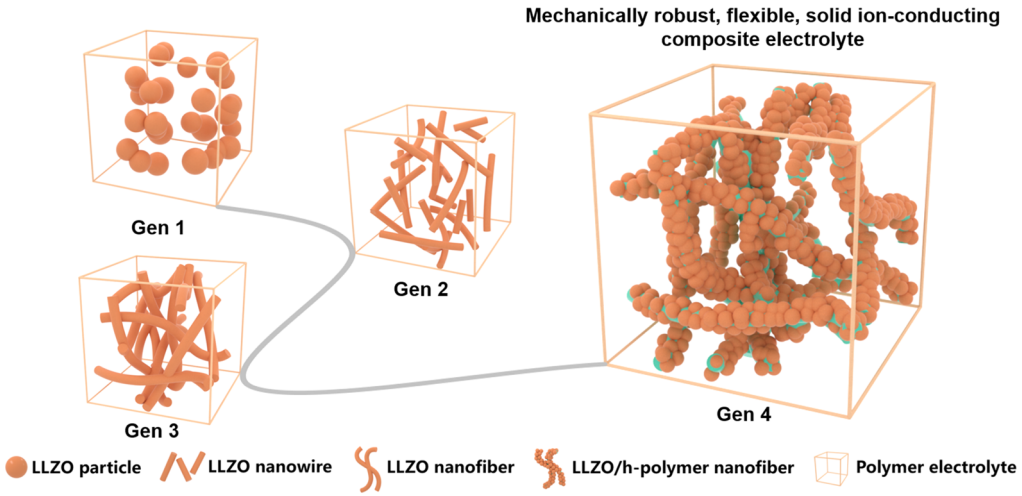

Figure 1. Schematic of inorganic/polymer composite solid electrolyte membrane evolution. Gen 1 is the composite electrolyte with discrete conducting oxide nanoparticles in polymer electrolyte. Gen 2 is the composite electrolyte with semidiscrete conducting oxide nanowires in polymer electrolyte. Gen 3 is the composite electrolyte with continuous but brittle conducting oxide 3D nanofiber network in polymer electrolyte. Gen 4 is this work: composite electrolyte developed in this work that uses continuous and mechanically robust conducting oxide-enhanced 3D polymer nanofiber network in polymer electrolyte.

extended ion transport paths created from conducting nanowire filler in polymer matrix, which is better than that of composite made from traditional isolated distributed nanoparticles.[22] Agglomeration issue and precipitation of fillers in polymer matrix may still challenge preparation of composite electrolyte membrane, and mechanically mixing may damage brittle ceramic nanowires as well. Another representative work reported by Fu et al. marks an advancement in solid composite electrolyte membrane.[32] A 3D ceramic network based on garnet $Li_7La_3Zr_2O_{12}$ (LLZO) ceramic fibers was synthesized and developed by creating a continuous ion transport pathway to overcome the issues that existed for isolated nanoparticles or nanowires, to achieve both electrochemical and mechanical reinforcement of conducting polymers. Since then, creating a continuous nanosized network with interconnected ion transport and controlling the minimum/nonfilled agglomeration has become the main effort in solid composite electrolyte membrane development.[33−36]

Although creating a garnet LLZO nanofiber 3D network has proved to be a promising strategy to transform solid-state electrolyte membrane with claimed enhancement in mechanical property, structural stability, and roll-to-roll manufacturing, there are many technical challenges in garnet LLZO nanofiber production and end-use.[32] LLZO ceramic nanofibers have to be performed in a well-controlled temperature and humidity condition to avoid water uptake in LLZO and ensure polyvinylpyrrolidone (PVP) nanofiber formation, and large dimension shrinkage during the "green part" sintering in the subsequent high-temperature LLZO crystallization process weakens the mechanical property of the "brown part", and the resulting brittle ceramic nanofiber structure makes it difficult to serve as a mechanical support during conducting polymer impregnation, battery fabrication, and end use. Many practical challenges as formerly mentioned have emerged but yet to be addressed, which largely hindered composite electrolyte membrane application in solid lithium battery. Therefore, in order to move forward with composite electrolyte membrane, the key is to develop a high mechanically robust 3D ion-conducting network to ionically reinforce the membrane.

To overcome the challenges that are mainly brought by the single use of ceramic nanomaterials, in this manuscript we reported a new 3D ion-conducting network, which is synthesized from highly loaded LLZO nanoparticles enhancing conducting polymer nanofibers, by creating a lightweight continuous and interconnected 3D network to outperform the current state-of-the-art conducting heavy and brittle ceramic nanofibers to offer a new design principle of composite electrolyte membrane featuring all-round properties in mechanical robustness, structural flexibility, high ionic conductivity, lightweight and high surface area. This conductive oxide-enhanced nanofiber design overcomes the issues of using ceramic-only nanoparticles, nanowires, or nanofibers in polymer composite electrolyte, and our work can be considered as a new generation of composite electrolyte membrane (Figure 1). A conductive binder containing polyvinylidene fluoride (PVDF) and poly(ethylene oxide) (PEO) hybrid with bis(trifluoromethane)sulfonimide lithium salt (LiTFSI) is developed to electrospin together with LLZO nanoparticles to form a LLZO-loaded 3D nanofiber network. The addition of LLZO not only mechanically reinforces the mechanical strength of nanofiber but also ionically reinforces the ionic conductivity of a 3D network, forming a continuous lithium ions pathway and promoting the transfer of lithium ions. Earlier study has revealed that the complexation of LLZO with *N*,*N*-dimethylformamide (DMF) can form an environment similar to Lewis bases and induce partial dehydrofluorination of the PVDF skeleton, thereby enhancing interactions with the PVDF matrix, lithium salt, and LLZO particles, which results in accelerating the salt decomposition of the lithium salt and improves the ion conductivity.[37] Using conducting PEO polymer electrolyte to impregnate into 3D conducting network could improve the electrolyte/electrode contact and structural stability. In addition, the 3D nanofiber could increase the amorphous region of PEO polymer electrolyte, and the synergistic effect of both polymers and garnet LLZO could enhance mechanical and ionic property. In this work, our composite electrolyte membrane has exhibited a high lithium ion transference number, wider electrochemical window, enhanced thermal conductivity, and interface stability

https://doi.org/10.1021/acs.nanolett.1c01704
Nano Lett. XXXX, XXX, XXX−XXX

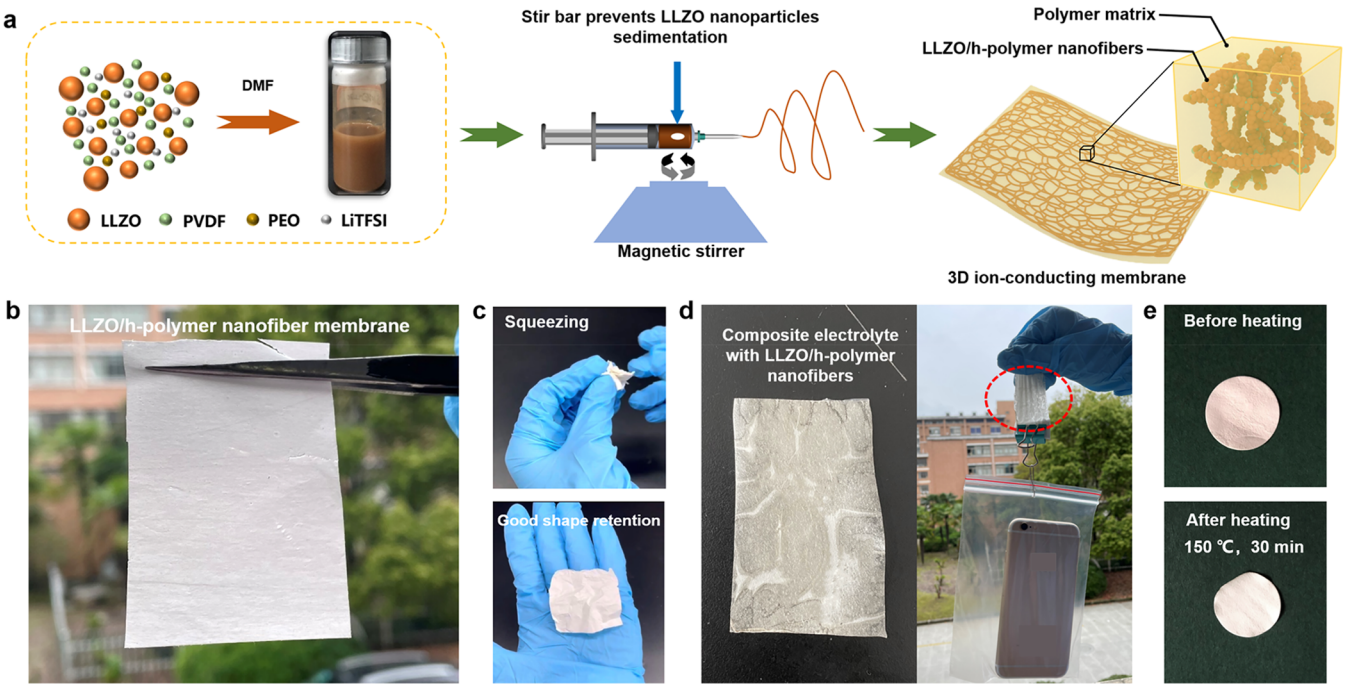

Figure 2. Preparation of solid electrolyte membrane using LLZO loaded polymeric nanofiber network. (a) Schematic diagram of the preparation of composite electrolyte with LLZO/h-polymer nanofibers. (b) Digital photo of LLZO/h-polymer nanofiber membrane. (c) Digital photos of LLZO/h-polymer nanofiber membrane squeezed into a cluster and before and after. (d) Digital photos of composite electrolyte with LLZO/h-polymer (PVDF−PEO with LiTFSI) nanofibers and its hanging mobile phone (inside the red circle). (e) Digital photos of composite electrolyte with LLZO/h-polymer (PVDF−PEO with LiTFSI) nanofibers before and after heating at 150 °C for 30 min.

with the lithium anode, representing an advancement in composite electrolyte development.

RESULTS AND DISCUSSION

A schematic illustration of the preparation of composite electrolyte with LLZO/h-polymer nanofibers is shown in Figure 2a. First, LLZO nanoparticles (SI Figure 1), PVDF polymer, PEO polymer, and LiTFSI salt were added to the DMF solvent and fully mixed to obtain the LLZO/h-polymer electrospinning solution, where h-polymer is termed as hybrid polymer containing PEO, PVDF, and LiTFSI. The small amount of PEO (5 wt %) acts as a plasticizer to reduce the crystallinity of PVDF and promote ion conduction.[38−40] Then the LLZO particles were spun together with h-polymer to form the 3D network. In this process, a stir bar continues to rotate under the action of magnetic force to prevent the sedimentation of LLZO nanoparticles, so that the nanoparticles can be completely spun into the nanofibers. This is a critical step to successfully make LLZO-loaded nanofibers. Figure 2b,c shows that the LLZO/h-polymer nanofiber membrane is light and thin while featuring excellent flexibility and mechanical robustness. After being squeezed into a cluster by external force, there is good shape retention in paving without damage. Finally, a mixed solution of PEO and LiTFSI was impregnated into LLZO/h-polymer nanofiber membrane and dried to obtain the composite electrolyte. As shown in Figure 2d, the electrolyte membrane with excellent mechanical property can lift up a phone (132.82 g) without tearing. In addition, the composite electrolyte with LLZO/h-polymer nanofibers will not deform after being heated at 150 °C for 30 min and only slightly shrink compared to the original shape (Figure 2e).

In Figure 3a, the schematic shows that LLZO/h-polymer nanofibers are interwoven into a three-dimensional network structure, and the cross-contact points between the fibers ensure the continuity of the lithium ions path and promote the efficient transmission of lithium ions. In a single fiber, h-polymers (PVDF−PEO with LiTFSI) act as a binder to interconnect LLZO particles together instead of fully covering or embedding LLZO particles to ensure a continuous ion transport path formed by LLZO particle contours. The morphology of LLZO/h-polymer nanofibers with 20 wt % LLZO loading (20-LLZO/h-polymer nanofibers) are shown in Figure 3b,c. Continuous fibers with evenly loaded LLZO particles are noticeable. The nanofiber has an average diameter of 700 nm. In the TEM image, we can see LLZO particles are interconnected, and a large fraction of particle are uncovered and not fully embedded in polymers. Such morphology is closed to an ideal design of LLZO-enhanced nanofiber structure, where large areas of LLZO could play a role of ionic-enhancement in solid electrolyte membrane after conductive polymer impregnation. In comparison, LLZO/h-polymer nanofibers with 10 and 30 wt % LLZO nanoparticles were prepared, and morphology with uneven fiber formation and particle agglomerates are observed (SI Figure 2).

The powder X-ray diffraction (XRD) patterns show that the characteristic peak of LLZO and PVDF appeared in the LLZO/h-polymer nanofibers at the same time after the introduction of LLZO (Figure 3e), demonstrating that they are fully mixed. To prove the good thermal stability of the electrolyte, thermogravimetric analysis (TGA) was carried out under airflow with a rapid heating rate of 20 °C min^{-1}. Figure 3f shows the TGA profile of h-polymer nanofibers and LLZO/h-polymer nanofibers. For the h-polymer nanofibers, the weight began to drop sharply when the temperature was

https://doi.org/10.1021/acs.nanolett.1c01704
Nano Lett. XXXX, XXX, XXX−XXX

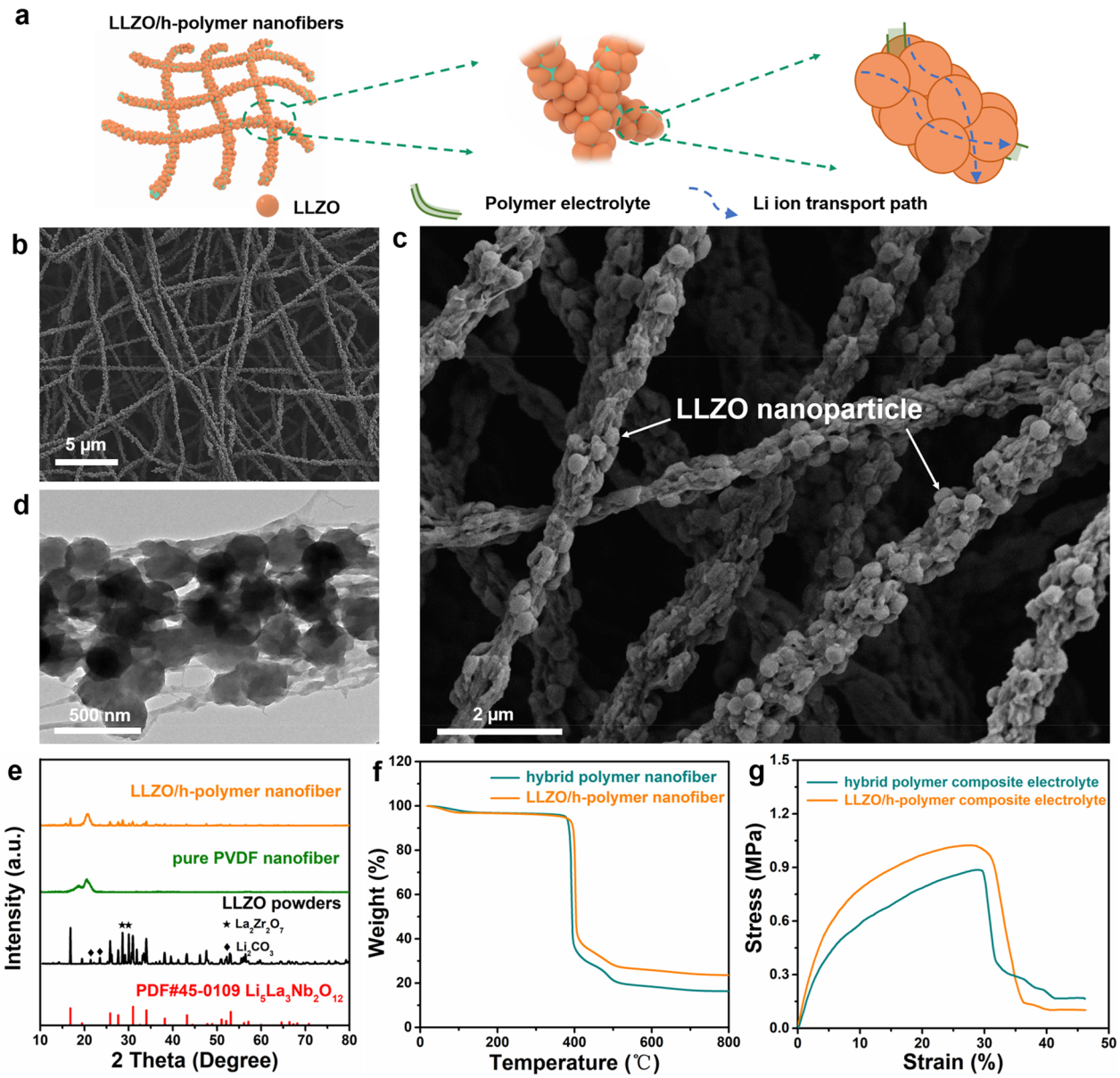

Figure 3. Morphology and structure characterization of 3D ion-conducting nanofiber networks. (a) Schematic diagram of the distribution of LLZO particles on hybrid polymer nanofibers. SEM images of LLZO/h-polymer nanofibers in the (b) low and (c) high magnification. (d) TEM images of LLZO/h-polymer nanofibers. (e) XRD pattern of LLZO powders, pure PVDF nanofibers, and LLZO/h-polymer nanofibers. (f) TGA of hybrid polymer (PVDF−PEO with LiTFSI) nanofibers and LLZO/h-polymer (PVDF−PEO with LiTFSI) nanofibers. (g) Stress−strain profiles of PEO-based composite electrolyte membrane with hybrid polymer (PVDF−PEO with LiTFSI) nanofibers and LLZO/h-polymer nanofibers as 3D network reinforcement, respectively.

approximately 352 °C, indicating that the nanofibers began to undergo thermal degradation. However, the weight of the LLZO/h-polymer nanofibers decreased significantly at 397 °C. The above results show that LLZO can impart thermal stability to the composite electrolyte, thereby improving the safety of the battery. The tensile strengths of composite electrolyte with h-polymer nanofibers and composite electrolyte with LLZO/h-polymer nanofibers were characterized by stress−strain curves. The composite electrolyte with LLZO/h-polymer nanofibers exhibit a high tensile strength of 1.03 MPa and modulus of 23.24 MPa with a maximum strain of 30.2%. (Figure 3g). In comparison, without LLZO enhancement the tensile strength is 0.88 MPa and modulus is 11.43 MPa.

The ionic conductivity (σ) curve of composite electrolyte with h-polymer nanofibers and composite electrolyte with LLZO/h-polymer nanofibers with different LLZO contents as a function of temperature was calculated using SI eq 1, leading to the following conclusions: as the content of LLZO in the composite electrolyte increases, the σ reaches a maximum when the LLZO content increases to 20% (Figure 4a). The σ of composite electrolyte with 20-LLZO/h-polymer nanofibers reach 1.05×10^{-4} S cm^{-1} at 50 °C (SI Figure 4), which is an order of magnitude higher than composite electrolyte with h-polymer nanofibers (2.53×10^{-5} S cm^{-1}) at the same temperature (SI Figure 5). This further proves that the optimal addition of LLZO is 20 wt %. The lithium ion transference number (t_{Li^+}) is a necessary factor for evaluating the ion transport capability of an electrolyte. The polarization current of the composite electrolyte with h-polymer nanofibers starts to decrease from 15.8 μA and remains stable at 6.85 μA (SI

https://doi.org/10.1021/acs.nanolett.1c01704
Nano Lett. XXXX, XXX, XXX−XXX

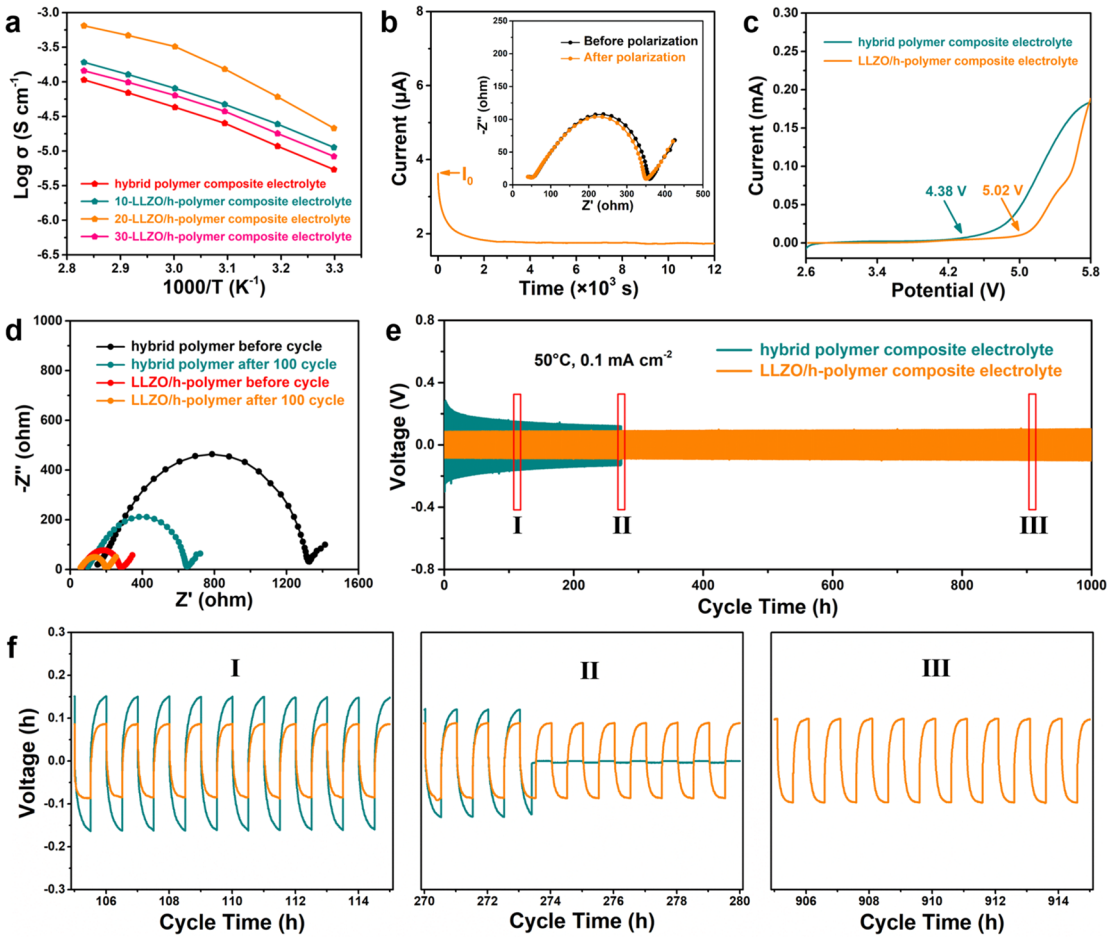

Figure 4. Electrochemical characterization of composite electrolyte with LLZO/h-polymer nanofibers. (a) Arrhenius curve of composite electrolyte with h-polymer nanofibers and composite electrolyte with LLZO/h-polymer nanofibers with different LLZO content. (b) Chronoamperometry profile of Li | LLZO/h-polymer|Li symmetric batteries; (inset) the Nyquist impedance spectra of batteries before and after polarization. (c) LSV curves of composite electrolyte with h-polymer nanofibers and composite electrolyte with LLZO/h-polymer nanofibers. (d) Electrochemical impedance of Li|h-polymer|Li and Li|LLZO/h-polymer|Li cells before and after cycle. (e) Cycling performance of Li/Li symmetric batteries with composite electrolyte with h-polymer nanofibers and composite electrolyte with LLZO/h-polymer nanofibers. (f) Enlarged view of cycle stages I, II, and III in (e).

Figure 6). The t_{Li^+} is 0.16. In contrast, the polarization current of the composite electrolyte with LLZO/h-polymer nanofibers start to drop from 3.63 μA and stabilizes at 1.76 μA (Figure 4b). The t_{Li^+} reaches 0.45 at 50 °C. On the one hand, the LLZO/h-polymer nanofibers form a 3D network structure with continuous lithium ions channels, optimizing the transmission of lithium ions. On the other hand, the interaction between the LLZO particles and DMF can cause the partial dehydrofluorination of PVDF.[37,42,43] In this process, PVDF molecular chain has more active areas that can further promote the interaction between PVDF, LLZO, and LiTFSI and accelerate the dissociation of lithium salt, thus providing more free lithium ions. In the Raman spectra, compared with the composite electrolyte with h-polymer nanofibers, the composite electrolyte with LLZO/h-polymer nanofibers have two new peaks at 1514 and 1121 cm^{-1} (SI Figure 7). These two peaks correspond to the stretching vibration of C=C in the PVDF mode, which demonstrates that dehydrofluorination occurred in the composite electrolyte with LLZO/h-polymer nanofibers.[41,44] LSV curves show the current value of composite electrolyte with h-polymer nanofibers suddenly rising at 4.68 V, indicating that the electrolyte has begun to decompose, while the composite electrolyte with LLZO/h-polymer nanofibers maintains a stable value between 2.6 and 5.02 V, which characterizes its electrochemical stability (Figure 4c). To further explore the stability of composite electrolyte with LLZO/h-polymer nanofibers with the lithium metal interface, EIS of Li|h-polymer|Li, Li|LLZO/h-polymer|Li batteries were tested before and after the cycle. The interface resistance of Li|h-polymer|Li battery decreased from 1327.6 to 648.5 Ω after cycling, while Li|LLZO/h-polymer|Li battery decreased from 282.4 to 199.2 Ω and stayed stable after 300 h of cycling (Figure 4d and SI Figure 8). The impedance of the composite electrolyte with LLZO/h-polymer nanofibers did not change significantly, suggesting that a stable electrolyte−lithium metal anode interface formed on account of the uniformly dispersed LLZO imparts excellent mechanical strength to the electrolyte, which renders the current density uniform while suppressing the growth of lithium dendrites. The Li|LLZO/h-polymer|Li symmetrical battery remained stable within 1000 h of cycling. No short circuit occurred after 1000 h and the polarization voltage remained stable at approximately 80 mV. This indicates good interface stability between the electrolyte and lithium metal. However, the Li|h-polymer|Li symmetrical battery had a large polarization voltage

https://doi.org/10.1021/acs.nanolett.1c01704
Nano Lett. XXXX, XXX, XXX−XXX

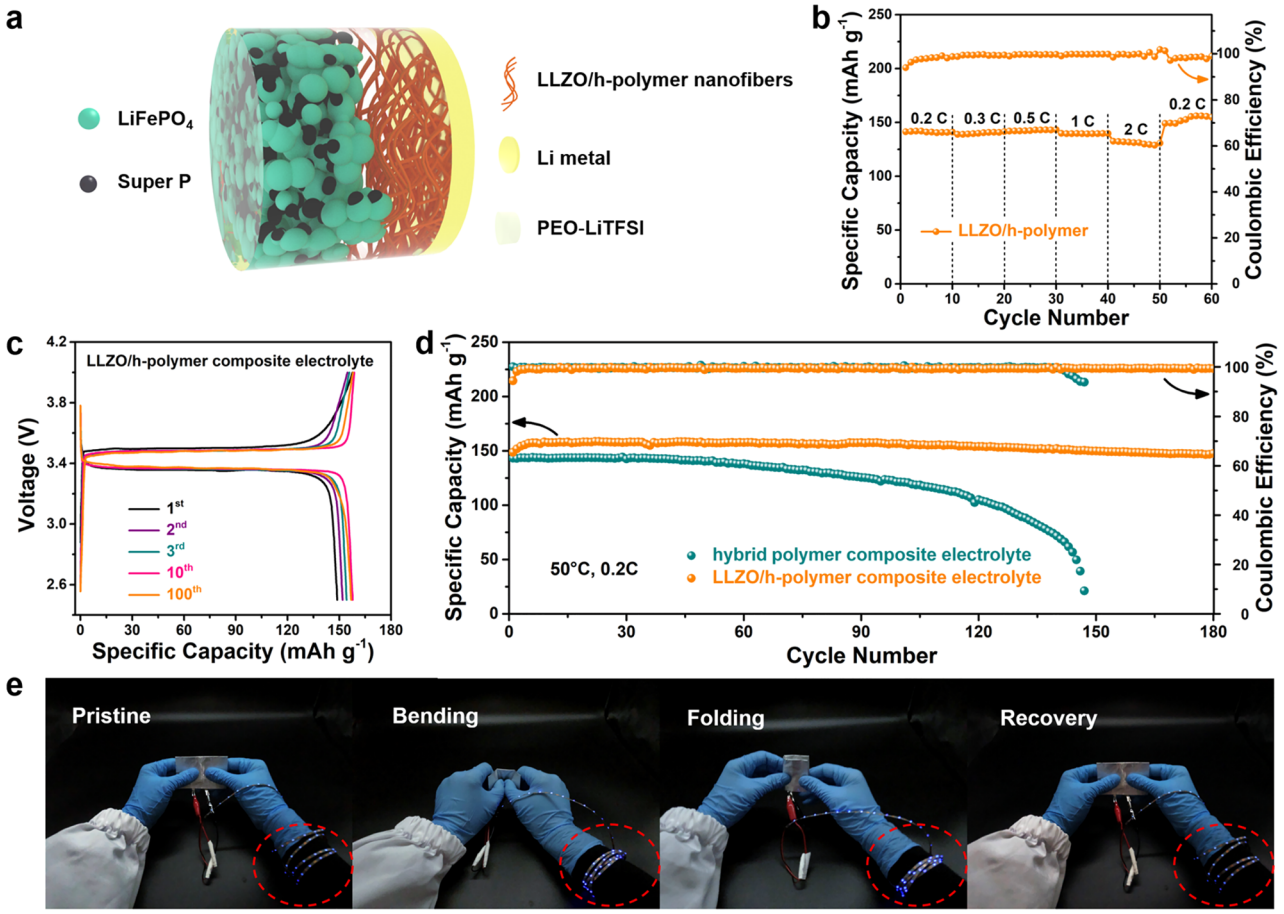

Figure 5. Characterization of cycle performance of the $LiFePO_4$/Li battery with composite electrolyte with LLZO/h-polymer nanofibers and flexibility characterization of composite electrolyte with LLZO/h-polymer nano)fibers. (a) Schematic of integrated $LiFePO_4$/Li battery with composite electrolyte with LLZO/h-polymer nanofibers. (b) Rate capacity (0.2−2 C) of $LiFePO_4$/Li batteries with composite electrolyte with LLZO/h-polymer nanofibers. (c) Charge and discharge curves of $LiFePO_4$|LLZO/h-polymer|Li battery at different number of cycles under 0.2 C at 50 °C. (d) Long-term cycling performances of $LiFePO_4$/Li batteries with composite electrolyte with h-polymer nanofibers and composite electrolyte with LLZO/h-polymer nanofibers under 0.2 C at 50 °C. (e) Optical images of original, bending, folding, and recovery tests of pouch-type $LiFePO_4$/Li cell with composite electrolyte with LLZO/h-polymer nanofibers. LED strips are marked with red circle.

in the initial stage, and a short circuit occurred after 273 h of cycling (Figure 4e,f).

$LiFePO_4$/Li batteries with composite electrolyte with LLZO/h-polymer nanofibers were assembled to characterize their applicability (Figure 5a). The PEO in the cathode and the composite electrolyte with LLZO/h-polymer nanofibers melt at high temperatures to form an integrated all-solid-state battery structure, which effectively enhances the compatibility and stability of the interface between the cathode and the composite electrolyte with LLZO/h-polymer nanofibers and ensures efficient ion transmission during long cycling. The schematic of the assembled all-solid-state battery is shown in SI Figure 9. Because of the continuous lithium ion transmission channel provided by the composite electrolyte with LLZO/h-polymer nanofibers, lithium ions can be quickly transferred in the all-solid-state battery system. The corresponding rate capacity of $LiFePO_4$/Li battery with the composite electrolyte with LLZO/h-polymer nanofibers at various current densities at 50 °C. It exhibits discharge capacities of 141.4, 141.5, 143.3, 139.7, and 130.8 mAh g^{-1} at different rates of 0.2, 0.3, 0.5, 1, and 2 C, respectively (Figure 5b). When the rate returns to 0.2 C, the specific capacity returns to 149 mAh g^{-1}, suggesting the excellent stability of the integrated all-solid-state $LiFePO_4$|LLZO/h-polymer|Li battery. The charge and discharge curves of the $LiFePO_4$|LLZO/h-polymer|Li battery after cycling at 0.2 C are shown in Figure 5c. The charge and discharge curves of the battery at different cycles are relatively flat. After the first, second, third, 10th, and 100th cycles, the discharge capacities of the battery are 148.8, 151.9, 154.3, 157.7, and 156.7 mA h g^{-1}, respectively. The excellent capacity retention rate (99.2%) and minimal polarization throughout the cycle indicate that the composite electrolyte with LLZO/h-polymer nanofibers apply to improve the overall electrochemical performance of the battery. Instead, the charge and discharge curves of the $LiFePO_4$|h-polymer|Li battery is relatively stable at the beginning, but the capacity decreases faster in the long cycle. After the 100th cycle, the discharge capacity of the battery decreases from 143.2 to 121.5 mA h g^{-1} (SI Figure 10). Furthermore, the long-term cycling performance of $LiFePO_4$/Li battery assembled with composite electrolyte with h-polymer nanofibers and composite electrolyte with LLZO/h-polymer nanofibers at 0.2 C was investigated (Figure 5d). It displayed an initial discharge specific capacity of 148.8 mA h g^{-1} with a high-capacity retention rate of 99.2% after 180 cycles, revealing the excellent interface stability between the composite electrolyte with LLZO/h-polymer nanofibers and the lithium anode during cycling. Moreover, the Coulombic efficiency of the battery reached 99.3% after cycling, indicating

https://doi.org/10.1021/acs.nanolett.1c01704
Nano Lett. XXXX, XXX, XXX−XXX

that the battery had excellent long-time cycle stability. In comparison, the composite electrolyte with h-polymer nanofibers exhibits poor cycle stability performance. After about 142 cycles, the discharge capacity of $LiFePO_4$|h-polymer|Li decreases to 66.2 mA h g^{-1} and the coulomb efficiency begins to decrease rapidly. In addition, electrochemical impedance plots of $LiFePO_4$/Li cell before and after a cycle of composite electrolyte with LLZO/h-polymer nanofibers are shown in SI Figure 11. The interface resistance decreased from 748.52 to 535.7 Ω after 5 cycles under 0.2 C at 50 °C and decreased to 490.56 Ω after 10 cycles, which further demonstrated the good contact and stability between the composite electrolyte with LLZO/h-polymer nanofibers and the electrode. The pouch-type $LiFePO_4$/Li cell was fabricated to exhibit the flexibility of the composite electrolyte with LLZO/h-polymer nanofibers and its functionality when applied to lithium metal batteries. The pouch cell could light on the LED strip under bending, folding, and after recovery (Figure 5e), demonstrating that the $LiFePO_4$|LLZO/h-polymer|Li pouch cell exhibits good flexibility and functionality.

CONCLUSION

In conclusion, a new conducting oxide-enhanced 3D ion-conducting network was developed featuring high mechanically robust, flexible, and ion-conducting properties, as well as higher specific surface area, consisting of interconnected conducting oxide nanoparticles (e.g., LLZO) and conducting polymer, as a mechanically robust alternative to many brittle conducting ceramic materials for solid Li battery. LLZO nanoparticles were synthesized and densely packed in polymer nanofibers by coelectrospinning with a hybrid polymer electrolyte (PVDF−PEO with LiTFSI) to form the 3D network. This structure not only enhances mechanical strength of the composite electrolyte but also further optimizes the transmission path of lithium ions. The electrochemical stable window is 5.02 V at 50 °C and ionic conductivity is 1.05×10^{-4} S cm^{-1} at 50 °C. Furthermore, the voltage of the Li/Li symmetric battery remained a stable cycling within 1000 h at 0.1 mA cm^{-2}. The all-solid-state batteries deliver a discharge specific capacity at 147.6 mAh g^{-1} and a capacity retention rate of 99.2% under 0.2 C after 180 cycles. This work provides a new advancement for polymer/inorganic solid electrolyte membrane and solid Li battery.

ASSOCIATED CONTENT

Supporting Information

The Supporting Information is available free of charge at https://pubs.acs.org/doi/10.1021/acs.nanolett.1c01704.

Details on experimental methods; materials characterizations, and electrochemical evaluation (PDF)

AUTHOR INFORMATION

Corresponding Authors

Yi Hu − *Key Laboratory of Advanced Textile Materials and Manufacturing Technology, Ministry of Education and Engineering Research Center for Eco-Dying and Finishing of Textiles, Ministry of Education, Zhejiang Sci-Tech University, Hangzhou 310018, P.R. China;* orcid.org/0000-0002-0912-3555; Email: huyi-v@zstu.edu.cn

Kun Kelvin Fu − *Department of Mechanical Engineering and Center for Composite Materials, University of Delaware, Newark, Delaware 19716, United States;* orcid.org/0000-0003-4963-615X; Email: kfu@udel.edu

Authors

Mengmeng Zhang − *Key Laboratory of Advanced Textile Materials and Manufacturing Technology, Ministry of Education and Engineering Research Center for Eco-Dying and Finishing of Textiles, Ministry of Education, Zhejiang Sci-Tech University, Hangzhou 310018, P.R. China*

Peng Pan − *Key Laboratory of Advanced Textile Materials and Manufacturing Technology, Ministry of Education and Engineering Research Center for Eco-Dying and Finishing of Textiles, Ministry of Education, Zhejiang Sci-Tech University, Hangzhou 310018, P.R. China*

Zhongling Cheng − *Key Laboratory of Advanced Textile Materials and Manufacturing Technology, Ministry of Education and Engineering Research Center for Eco-Dying and Finishing of Textiles, Ministry of Education, Zhejiang Sci-Tech University, Hangzhou 310018, P.R. China*

Jieting Mao − *Key Laboratory of Advanced Textile Materials and Manufacturing Technology, Ministry of Education and Engineering Research Center for Eco-Dying and Finishing of Textiles, Ministry of Education, Zhejiang Sci-Tech University, Hangzhou 310018, P.R. China*

Liyuan Jiang − *Key Laboratory of Advanced Textile Materials and Manufacturing Technology, Ministry of Education and Engineering Research Center for Eco-Dying and Finishing of Textiles, Ministry of Education, Zhejiang Sci-Tech University, Hangzhou 310018, P.R. China*

Changke Ni − *Key Laboratory of Advanced Textile Materials and Manufacturing Technology, Ministry of Education and Engineering Research Center for Eco-Dying and Finishing of Textiles, Ministry of Education, Zhejiang Sci-Tech University, Hangzhou 310018, P.R. China*

Soyeon Park − *Department of Mechanical Engineering and Center for Composite Materials, University of Delaware, Newark, Delaware 19716, United States*

Kaiyue Deng − *Department of Mechanical Engineering and Center for Composite Materials, University of Delaware, Newark, Delaware 19716, United States*

Complete contact information is available at: https://pubs.acs.org/10.1021/acs.nanolett.1c01704

Notes

The authors declare no competing financial interest.

ACKNOWLEDGMENTS

This work was supported by the Fundamental Research Funds of Zhejiang Sci-Tech University (2020Y001), the Zhejiang Provincial Natural Science Foundation of China (LY21E030023), Suzhou Shi Yuanfan Dianqi Co., LTD (17010291-J), the Fundamental Research Funds of Shaoxing Keqiao Research Institute of Zhejiang Sci-Tech University (KYY2021006Y), and University of Delaware startup funding.

REFERENCES

(1) Wang, C.; Fu, K.; Kammampata, S. P.; McOwen, D. W.; Samson, A. J.; Zhang, L.; Hitz, G. T.; Nolan, A. M.; Wachsman, E. D.; Mo, Y.; Thangadurai, V.; Hu, L. Garnet-Type Solid-State Electrolytes: Materials, Interfaces, and Batteries. *Chem. Rev.* **2020**, *120* (10), 4257−4300.

(2) Yang, C.; Fu, K.; Zhang, Y.; Hitz, E.; Hu, L. Protected Lithium-Metal Anodes in Batteries: From Liquid to Solid. *Adv. Mater.* **2017**, *29* (36), 1701169.
(3) Cheng, X.-B.; Zhang, R.; Zhao, C.-Z.; Wei, F.; Zhang, J.-G.; Zhang, Q. A Review of Solid Electrolyte Interphases on Lithium Metal Anode. *Adv. Sci.* **2016**, *3* (3), 1500213.
(4) Lin, D.; Liu, Y.; Cui, Y. Reviving the lithium metal anode for high-energy batteries. *Nat. Nanotechnol.* **2017**, *12* (3), 194−206.
(5) Tarascon, J. M.; Armand, M. Issues and challenges facing rechargeable lithium batteries. *Nature* **2001**, *414* (6861), 359−367.
(6) Xin, S.; You, Y.; Wang, S.; Gao, H.-C.; Yin, Y.-X.; Guo, Y.-G. Solid-State Lithium Metal Batteries Promoted by Nanotechnology: Progress and Prospects. *ACS Energy Lett.* **2017**, *2* (6), 1385−1394.
(7) Sun, Y.; Liu, N.; Cui, Y. Promises and challenges of nanomaterials for lithium-based rechargeable batteries. *Nat. Energy* **2016**, *1* (7), 16071.
(8) Xu, W.; Wang, J.; Ding, F.; Chen, X.; Nasybulin, E.; Zhang, Y.; Zhang, J.-G. Lithium metal anodes for rechargeable batteries. *Energy Environ. Sci.* **2014**, *7* (2), 513−537.
(9) Lin, D.; Zhuo, D.; Liu, Y.; Cui, Y. All-Integrated Bifunctional Separator for Li Dendrite Detection via Novel Solution Synthesis of a Thermostable Polyimide Separator. *J. Am. Chem. Soc.* **2016**, *138* (34), 11044−11050.
(10) Yu, B.-C.; Park, K.; Jang, J.-H.; Goodenough, J. B. Cellulose-Based Porous Membrane for Suppressing Li Dendrite Formation in Lithium-Sulfur Battery. *ACS Energy Lett.* **2016**, *1* (3), 633−637.
(11) Wu, H.; Zhuo, D.; Kong, D.; Cui, Y. Improving battery safety by early detection of internal shorting with a bifunctional separator. *Nat. Commun.* **2014**, *5* (1), 5193.
(12) Wood, K. N.; Kazyak, E.; Chadwick, A. F.; Chen, K.-H.; Zhang, J.-G.; Thornton, K.; Dasgupta, N. P. Dendrites and Pits: Untangling the Complex Behavior of Lithium Metal Anodes through Operando Video Microscopy. *ACS Cent. Sci.* **2016**, *2* (11), 790−801.
(13) Fu, K. K.; Gong, Y.; Xu, S.; Zhu, Y.; Li, Y.; Dai, J.; Wang, C.; Liu, B.; Pastel, G.; Xie, H.; Yao, Y.; Mo, Y.; Wachsman, E.; Hu, L. Stabilizing the Garnet Solid-Electrolyte/Polysulfide Interface in Li-S Batteries. *Chem. Mater.* **2017**, *29* (19), 8037−8041.
(14) Chang, H. J.; Ilott, A. J.; Trease, N. M.; Mohammadi, M.; Jerschow, A.; Grey, C. P. Correlating Microstructural Lithium Metal Growth with Electrolyte Salt Depletion in Lithium Batteries Using 7Li MRI. *J. Am. Chem. Soc.* **2015**, *137* (48), 15209−15216.
(15) Zhou, W.; Wang, S.; Li, Y.; Xin, S.; Manthiram, A.; Goodenough, J. B. Plating a Dendrite-Free Lithium Anode with a Polymer/Ceramic/Polymer Sandwich Electrolyte. *J. Am. Chem. Soc.* **2016**, *138* (30), 9385−9388.
(16) Li, Y.; Zhou, W.; Xin, S.; Li, S.; Zhu, J.; Lü, X.; Cui, Z.; Jia, Q.; Zhou, J.; Zhao, Y.; Goodenough, J. B. Fluorine-Doped Antiperovskite Electrolyte for All-Solid-State Lithium-Ion Batteries. *Angew. Chem., Int. Ed.* **2016**, *55* (34), 9965−9968.
(17) Wang, C.; Gong, Y.; Liu, B.; Fu, K.; Yao, Y.; Hitz, E.; Li, Y.; Dai, J.; Xu, S.; Luo, W.; Wachsman, E. D.; Hu, L. Conformal, Nanoscale ZnO Surface Modification of Garnet-Based Solid-State Electrolyte for Lithium Metal Anodes. *Nano Lett.* **2017**, *17* (1), 565−571.
(18) Liu, S.; Imanishi, N.; Zhang, T.; Hirano, A.; Takeda, Y.; Yamamoto, O.; Yang, J. Effect of nano-silica filler in polymer electrolyte on Li dendrite formation in Li/poly(ethylene oxide)-$Li(CF_3SO_2)_2N$/Li. *J. Power Sources* **2010**, *195* (19), 6847−6853.
(19) Damen, L.; Hassoun, J.; Mastragostino, M.; Scrosati, B. Solid-state, rechargeable Li/$LiFePO_4$ polymer battery for electric vehicle application. *J. Power Sources* **2010**, *195* (19), 6902−6904.
(20) Gurevitch, I.; Buonsanti, R.; Teran, A. A.; Gludovatz, B.; Ritchie, R. O.; Cabana, J.; Balsara, N. P. Nanocomposites of Titanium Dioxide and Polystyrene-Poly(ethylene oxide) Block Copolymer as Solid-State Electrolytes for Lithium Metal Batteries. *J. Electrochem. Soc.* **2013**, *160* (9), A1611−A1617.
(21) Choi, J.-H.; Lee, C.-H.; Yu, J.-H.; Doh, C.-H.; Lee, S.-M. Enhancement of ionic conductivity of composite membranes for all-solid-state lithium rechargeable batteries incorporating tetragonal $Li_7La_3Zr_2O_{12}$ into a polyethylene oxide matrix. *J. Power Sources* **2015**, *274*, 458−463.
(22) Liu, W.; Liu, N.; Sun, J.; Hsu, P.-C.; Li, Y.; Lee, H.-W.; Cui, Y. Ionic Conductivity Enhancement of Polymer Electrolytes with Ceramic Nanowire Fillers. *Nano Lett.* **2015**, *15* (4), 2740−2745.
(23) Zhang, J.; Zhao, N.; Zhang, M.; Li, Y.; Chu, P. K.; Guo, X.; Di, Z.; Wang, X.; Li, H. Flexible and ion-conducting membrane electrolytes for solid-state lithium batteries: Dispersion of garnet nanoparticles in insulating polyethylene oxide. *Nano Energy* **2016**, *28*, 447−454.
(24) Yao, P.; Yu, H.; Ding, Z.; Liu, Y.; Lu, J.; Lavorgna, M.; Wu, J.; Liu, X. Review on Polymer-Based Composite Electrolytes for Lithium Batteries. *Front. Chem.* **2019**, *7*, 522 DOI: 10.3389/fchem.2019.00522.
(25) Manuel Stephan, A.; Nahm, K. S. Review on composite polymer electrolytes for lithium batteries. *Polymer* **2006**, *47* (16), 5952−5964.
(26) Yang, L.; Lu, Z.; Qin, Y.; Wu, C.; Fu, C.; Gao, Y.; Liu, J.; Jiang, L.; Du, Z.; Xie, Z.; Li, Z.; Kong, F.; Yin, G. Interrelated interfacial issues between a $Li_7La_3Zr_2O_{12}$-based garnet electrolyte and Li anode in the solid-state lithium battery: a review. *J. Mater. Chem. A* **2021**, *9* (10), 5952−5979.
(27) Croce, F.; Appetecchi, G. B.; Persi, L.; Scrosati, B. Nanocomposite polymer electrolytes for lithium batteries. *Nature* **1998**, *394* (6692), 456−458.
(28) Yu, X.; Manthiram, A. A review of composite polymer-ceramic electrolytes for lithium batteries. *Energy Stor. Mater.* **2021**, *34*, 282−300.
(29) Wan, Z.; Lei, D.; Yang, W.; Liu, C.; Shi, K.; Hao, X.; Shen, L.; Lv, W.; Li, B.; Yang, Q.-H.; Kang, F.; He, Y.-B. Low Resistance-Integrated All-Solid-State Battery Achieved by $Li_7La_3Zr_2O_{12}$ Nanowire Upgrading Polyethylene Oxide (PEO) Composite Electrolyte and PEO Cathode Binder. *Adv. Funct. Mater.* **2019**, *29* (1), 1805301.
(30) Chen, W.-P.; Duan, H.; Shi, J.-L.; Qian, Y.; Wan, J.; Zhang, X.-D.; Sheng, H.; Guan, B.; Wen, R.; Yin, Y.-X.; Xin, S.; Guo, Y.-G.; Wan, L.-J. Bridging Interparticle Li^+ Conduction in a Soft Ceramic Oxide Electrolyte. *J. Am. Chem. Soc.* **2021**, *143* (15), 5717−5726.
(31) Walle, K. Z.; Musuvadhi Babulal, L.; Wu, S. H.; Chien, W.-C.; Jose, R.; Lue, S. J.; Chang, J.-K.; Yang, C.-C. Electrochemical Characteristics of a Polymer/Garnet Trilayer Composite Electrolyte for Solid-State Lithium-Metal Batteries. *ACS Appl. Mater. Interfaces* **2021**, *13* (2), 2507−2520.
(32) Fu, K.; Gong, Y.; Dai, J.; Gong, A.; Han, X.; Yao, Y.; Wang, C.; Wang, Y.; Chen, Y.; Yan, C.; Li, Y.; Wachsman, E. D.; Hu, L. Flexible, solid-state, ion-conducting membrane with 3D garnet nanofiber networks for lithium batteries. *Proc. Natl. Acad. Sci. U. S. A.* **2016**, *113* (26), 7094.
(33) Zhao, Y.; Yan, J.; Cai, W.; Lai, Y.; Song, J.; Yu, J.; Ding, B. Elastic and well-aligned ceramic LLZO nanofiber based electrolytes for solid-state lithium batteries. *Energy Stor. Mater.* **2019**, *23*, 306−313.
(34) Liu, Q.; Geng, Z.; Han, C.; Fu, Y.; Li, S.; He, Y.-b.; Kang, F.; Li, B. Challenges and perspectives of garnet solid electrolytes for all solid-state lithium batteries. *J. Power Sources* **2018**, *389*, 120−134.
(35) Li, Y.; Zhang, W.; Dou, Q.; Wong, K. W.; Ng, K. M. $Li_7La_3Zr_2O_{12}$ ceramic nanofiber-incorporated composite polymer electrolytes for lithium metal batteries. *J. Mater. Chem. A* **2019**, *7* (7), 3391−3398.
(36) Wang, X.; Zhang, Y.; Zhang, X.; Liu, T.; Lin, Y.-H.; Li, L.; Shen, Y.; Nan, C.-W. Lithium-Salt-Rich PEO/$Li_{0.3}La_{0.557}TiO_3$ Interpenetrating Composite Electrolyte with Three-Dimensional Ceramic Nano-Backbone for All-Solid-State Lithium-Ion Batteries. *ACS Appl. Mater. Interfaces* **2018**, *10* (29), 24791−24798.
(37) Zhang, X.; Liu, T.; Zhang, S.; Huang, X.; Xu, B.; Lin, Y.; Xu, B.; Li, L.; Nan, C.-W.; Shen, Y. Synergistic Coupling between $Li_{6.75}La_3Zr_{1.75}Ta_{0.25}O_{12}$ and Poly(vinylidene fluoride) Induces High Ionic Conductivity, Mechanical Strength, and Thermal Stability of Solid Composite Electrolytes. *J. Am. Chem. Soc.* **2017**, *139* (39), 13779−13785.

https://doi.org/10.1021/acs.nanolett.1c01704
Nano Lett. XXXX, XXX, XXX−XXX

(38) Prabakaran, P.; Manimuthu, R. P.; Gurusamy, S.; Sebasthiyan, E. Plasticized polymer electrolyte membranes based on PEO/PVdF-HFP for use as an effective electrolyte in lithium-ion batteries. *Chin. J. Polym. Sci.* **2017**, *35* (3), 407−421.
(39) Das, S.; Ghosh, A. Charge Carrier Relaxation in Different Plasticized PEO/PVDF-HFP Blend Solid Polymer Electrolytes. *J. Phys. Chem. B* **2017**, *121* (21), 5422−5432.
(40) Li, Z.; Xu, Y.; Fan, L.; Kang, W.; Cheng, B. Fabrication of polyvinylidene fluoride tree-like nanofiber via one-step electrospinning. *Mater. Des.* **2016**, *92*, 95−101.
(41) Zhang, S.; Shen, J.; Qiu, X.; Weng, D.; Zhu, W. ESR and vibrational spectroscopy study on poly(vinylidene fluoride) membranes with alkaline treatment. *J. Power Sources* **2006**, *153* (2), 234−238.
(42) Hashim, N. A.; Liu, Y.; Li, K. Preparation of PVDF Hollow Fiber Membranes Using SiO_2 Particles: The Effect of Acid and Alkali Treatment on the Membrane Performances. *Ind. Eng. Chem. Res.* **2011**, *50* (5), 3035−3040.
(43) Sinirlioglu, D.; Muftuoglu, A. E.; Golcuk, K.; Bozkurt, A. Investigation of proton conductivity of anhydrous proton exchange membranes prepared via grafting vinyltriazole onto alkaline-treated PVDF. *J. Polym. Sci., Part A: Polym. Chem.* **2014**, *52* (13), 1885−1897.
(44) Bottino, A.; Capannelli, G.; Monticelli, O.; Piaggio, P. Poly(vinylidene fluoride) with improved functionalization for membrane production. *J. Membr. Sci.* **2000**, *166* (1), 23−29.

https://doi.org/10.1021/acs.nanolett.1c01704
Nano Lett. XXXX, XXX, XXX−XXX